



# Targeting the Tat-Binding Site of Bovine Immunodeficiency Virus TAR RNA with a Shape-Selective Rhodium Complex

Ai Ching Lim and Jacqueline K. Barton\*

*Division of Chemistry and Chemical Engineering, California Institute of Technology, Pasadena, CA 91125, U.S.A.*

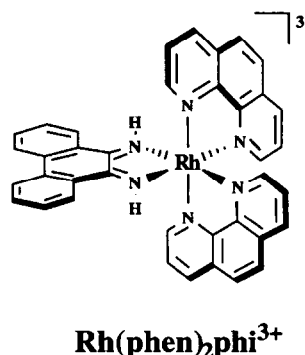
**Abstract**—The Tat-binding site of the bovine immunodeficiency virus TAR RNA hairpin has been targeted by  $\text{Rh}(\text{phen})_2\text{phi}^{3+}$  (phen = phenanthroline, phi = 9,10-phenanthrenequinone diimine), a photochemical probe of RNA tertiary structure. The primary site cleaved by the rhodium complex, upon photoactivation, is U24, a base which participates in the novel base triple (with bases A13 and U10) characteristic of this folded RNA.  $\Delta\text{-Rh}(\text{phen})_2\text{phi}^{3+}$  binds to this site with an affinity of  $2 \times 10^6 \text{ M}^{-1}$ . Upon mutation of U24 and A13 to A24 and U13, respectively, so that the RNA oligomer is unable to form the base triple, site-specific cleavage by the rhodium complex is abolished. Moreover, as determined through rhodium photocleavage, at a concentration of 20  $\mu\text{M}$ ,  $\text{Rh}(\text{phen})_2\text{phi}^{3+}$  inhibits specific binding of BIV-Tat peptide (2  $\mu\text{M}$ ) to its target site. Thus the rhodium complex, in matching its shape to the opened major groove of the properly folded RNA, specifically targets its site and is able to compete for its target with the BIV-Tat peptide. © 1997 Elsevier Science Ltd.

The *trans*-activating (Tat) protein of bovine immunodeficiency virus (BIV) binds the *trans*-activation response (TAR) RNA hairpin element located at the 5'-end of the viral mRNA and thereby activates transcription.<sup>1</sup> Recognition of this RNA site has been found to depend upon the folding of the RNA into a remarkable structure in which an intramolecular base triple is formed and the RNA major groove is widened to accept the Tat  $\beta$ -hairpin peptide. Recent high-resolution NMR studies<sup>2,3</sup> have served to elucidate specific contacts between the RNA bases and amino acids of the Tat peptide in the opened major groove of RNA. Additionally, NMR data have been used to establish the intramolecular base triple, U10-A13-U24, in the presence of specifically bound Tat peptides.<sup>3</sup> Bases involved in maintaining this fold have furthermore been found to be essential for *in vivo* expression.<sup>1</sup> This interesting RNA fold resembles that found by NMR<sup>4</sup> in the recognition of human immunodeficiency viral (HIV) TAR RNA by its associated Tat protein, despite differences in the structure and sequences of the RNA bulge and loop region.<sup>1</sup>

Our interest is in the design of octahedral transition metal complexes which bind nucleic acids with site-selectivity.<sup>5</sup> Illustrated schematically, below, is the complex  $\text{Rh}(\text{phen})_2\text{phi}^{3+}$ , which serves as a site-selective probe of RNA tertiary structure (Scheme 1).

This complex binds to DNA duplexes by intercalation in the major groove.<sup>6</sup> The complex shows no detectable binding to A-conformational RNA duplexes, which contains a narrow and deepened major groove, but instead targets sites of triple base interactions, or other local RNA conformations which serve to open the major groove, allowing access of the intercalator.<sup>7</sup> Site-selective binding is marked through direct strand

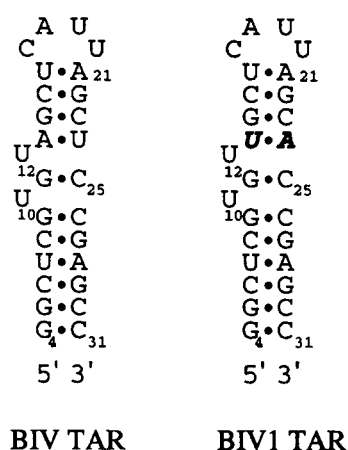
cleavage upon photoactivation.<sup>8</sup> On tRNAs,  $\text{Rh}(\text{phen})_2\text{phi}^{3+}$  has been shown specifically to target only sites involved in tertiary interactions.<sup>9</sup> Mutations which disrupt RNA folding disrupt targeting by the metal complex, but base changes which maintain folding also maintain site-specific reaction. With double-stranded DNA, where the major groove is more accessible to intercalation than an A-form duplex, shape-selective binding and cleavage is observed at pyrimidine-pyrimidine-purine sites, those which are somewhat opened in the major groove.<sup>10</sup> Photocleavage experiments have also been conducted on tDNA, and here both sites of tertiary interaction and double helical regions are targeted; these results reflect the similarity in folding of tRNA and tDNA but the conformational difference, A-form versus B-form, between the two in duplex regions.<sup>11</sup> Based upon the unique shape-selective targeting by  $\text{Rh}(\text{phen})_2\text{phi}^{3+}$ , the metal complex has already been applied in probing HIV TAR RNA.<sup>12</sup> Here, as well, site-specific cleavage is evident neighboring the site of RNA tertiary interaction within the



Scheme 1.

opened major groove. Interestingly, for this RNA, adoption of the folded base triple has been found to be induced by binding of HIV Tat peptide; site-specific cleavage by the metal complex does not, however, require Tat peptide and may instead serve to drive the conformational change to the folded RNA element.

Here we describe the site-specific targeting of BIV TAR RNA by  $\text{Rh}(\text{phen})_2\text{phi}^{3+}$ . The shape-selective metal complex is found to target the triple base site with an affinity of  $10^6 \text{ M}^{-1}$ , and this site-specific binding is found to depend upon formation of the triple base interaction. While specific cleavage is induced by the rhodium complex with photocleavage at U24, no comparable targeting is found on BIV1 TAR RNA, which does not adopt the folded conformation involving a base triple.



Furthermore, we demonstrate that binding to this site by the metal complex can compete with specific binding of the Tat peptide. Hence, this shape-selective targeting may provide a route not only to probe RNA structures but also to inhibit RNA function.

## Results

### Site-specific photocleavage of BIV TAR RNA by $\text{Rh}(\text{phen})_2\text{phi}^{3+}$

Figure 1 shows the rhodium-induced cleavage with photoactivation of the BIV TAR RNA. At micromolar concentrations of rhodium, primary cleavage is evident at U24, a base involved in the triple interaction in the presence of the BIV Tat peptide.<sup>3</sup> With increasing concentration of rhodium, some cleavage is also found over the controls at G9, neighboring the open bulge site. Still weaker cleavage is evident in the hairpin loop at U20 and C17 at high rhodium concentration ( $> 10 \mu\text{M}$ ). It should be noted in these studies with synthetic RNAs that nuclease activity could not be eliminated. Nonetheless, data taken as a function of rhodium concentration make quite apparent the rhodium-induced sites of cleavage.

This specific targeting of the site of tertiary interaction in the RNA is enantiospecific. No similar site-specific cleavage is found with  $\Delta\text{-Rh}(\text{phen})_2\text{phi}^{3+}$ . It is interesting that recent studies in our laboratory of the targeting of HIV TAR RNA by enantiomers of  $\text{Rh}(\text{phen})_2\text{phi}^{3+}$  show no similar enantioselectivity in cleavage.<sup>13</sup> Perhaps this reflects a tighter, more restricted site for the rhodium complex on BIV TAR RNA compared to HIV TAR RNA.

A direct demonstration that targeting by the rhodium complex of the site of tertiary interaction depends upon the formation of the base triple can be seen in comparing photocleavage on BIV TAR RNA to that on BIV1 TAR RNA, in which base triple formation is precluded. This mutation yields a 75% loss of binding affinity to the Tat peptide and a 93% loss of activation

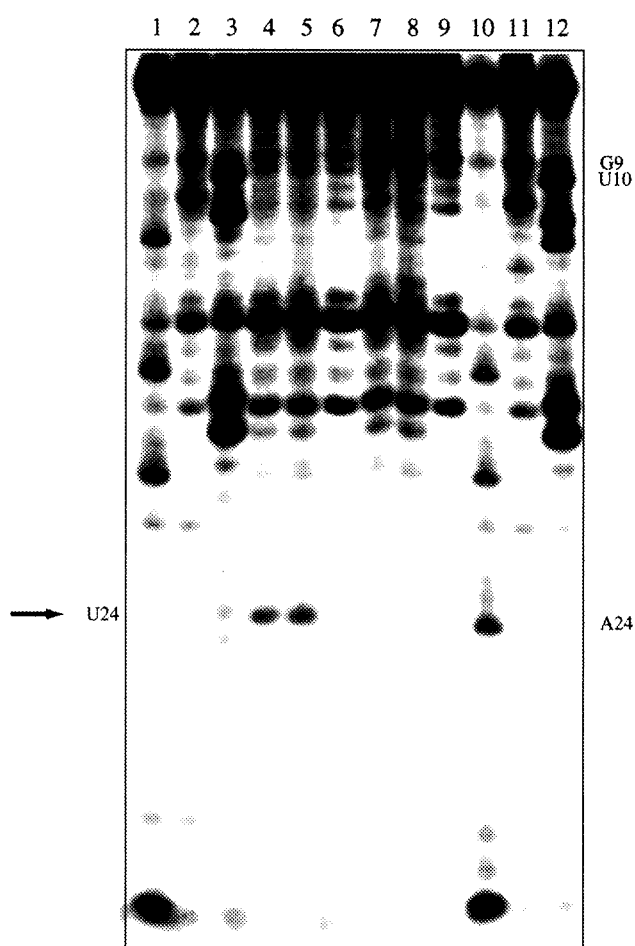


**Figure 1.** Gray-scale representation of a phosphor autoradiogram of a 20% denaturing polyacrylamide gel showing  $\Delta\text{-Rh}(\text{phen})_2\text{phi}^{3+}$  cleavage on  $3'\text{-}^{32}\text{P}$ -labeled BIV (lanes 1–6) and BIV1 RNA (lanes 7–12) in 50 mM Tris-HCl, 18 mM NaCl, 10 mM NaOAc, pH 7.0. Lanes 1, 2, and 3: A-, G-, and U-specific reactions on BIV, respectively. Lanes 4 and 5: labeled BIV after incubation with 1 and 5  $\mu\text{M}$   $\Delta\text{-Rh}(\text{phen})_2\text{phi}^{3+}$ , respectively, and irradiation for 15 min at 365 nm. Lane 6: labeled BIV upon irradiation for 15 min at 365 nm without metal complex. Lanes 7 and 8: labeled BIV1 after incubation with 1 and 5  $\mu\text{M}$   $\Delta\text{-Rh}(\text{phen})_2\text{phi}^{3+}$ , respectively, and irradiation for 15 min at 365 nm. Lane 9: labeled BIV1 upon irradiation for 15 min at 365 nm without metal complex. Lanes 10, 11, and 12: A-, G-, and U-specific reactions on BIV1, respectively.

in vivo.<sup>1</sup> As is evident in Figure 1 (lanes 7 and 8), incubation and irradiation of  $\Delta$ -Rh(phen)<sub>2</sub>phi<sup>3+</sup> with BIV1 yields no specific cleavage at A24. Interestingly, some cleavage is still evident on this RNA hairpin at G9 and to a lesser extent at U10. Likely the bulged RNA is sufficiently open to allow some access by the rhodium complex into a major groove site.

Measurements of photocleavage as a function of absolute concentration of rhodium/BIV TAR RNA allow the determination of the binding affinity of Rh(phen)<sub>2</sub>phi<sup>3+</sup> to its target site. Figure 2 shows this binding titration for Rh(phen)<sub>2</sub>phi<sup>3+</sup> based upon quantitative photocleavage at U24. The data indicate an affinity constant,  $K_b = 2.2 \pm 0.3 \times 10^6 \text{ M}^{-1}$  for Rh(phen)<sub>2</sub>phi<sup>3+</sup> to its target site on BIV TAR RNA.

### Competition between Rh(phen)<sub>2</sub>phi<sup>3+</sup> and BIV Tat-14

Arginine-rich 14-mer and 9-mer peptides derived from BIV Tat and HIV Tat, respectively, were chemically synthesized in order to carry out competition experiments between these Tat peptides and Rh(phen)<sub>2</sub>phi<sup>3+</sup> for BIV TAR RNA. Figure 3 shows the results of photocleavage by Rh(phen)<sub>2</sub>phi<sup>3+</sup> on BIV TAR RNA in the presence and absence of either HIV Tat peptide and BIV Tat peptide. As can be seen in Figure 3, despite its high arginine content, the HIV Tat peptide does not compete effectively with Rh(phen)<sub>2</sub>phi<sup>3+</sup>. Specific photocleavage of U24 is evident by the rhodium complex in the presence of micromolar concentrations of rhodium complex. This is despite the fact that the HIV Tat peptide has an affinity for BIV TAR RNA in the micromolar regime.<sup>1</sup>

Tighter specific binding of BIV Tat peptide to its target BIV RNA than to the HIV counterpart is evident.<sup>1</sup>

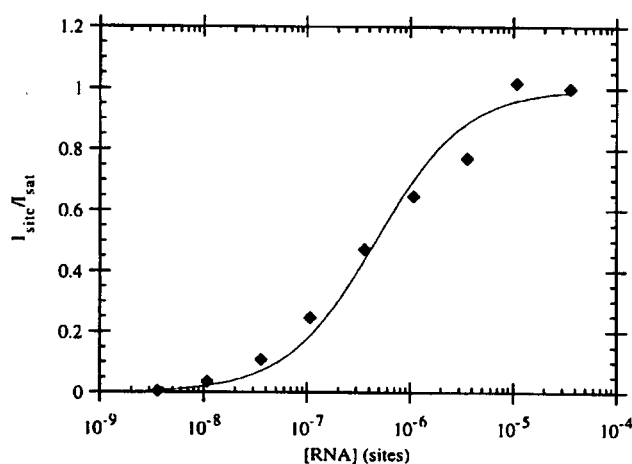


**Figure 2.** Quantitative affinity cleavage titration for Rh(phen)<sub>2</sub>phi<sup>3+</sup> on BIV RNA. Plot of cleavage intensity,  $I_{\text{site}}$ , relative to the intensity at saturation,  $I_{\text{sat}}$ , as a function of RNA concentration. These data represent the site-specific cleavage signal intensity at U24 with a Rh:BIV TAR RNA ratio of 1:1. Experiments were conducted at ambient temperature in 50 mM Tris-HCl, 18 mM NaCl, 10 mM NaOAc, pH 7.0, buffer, with irradiation at 365 nm.

Affinities of the BIV Tat peptide for BIV TAR RNA have been previously reported to be  $2 \times 10^8 \text{ M}^{-1}$ .<sup>1</sup> At stoichiometric rhodium and BIV Tat peptide concentrations, no specific cleavage by the rhodium complex is therefore evident. Given its lower affinity for the RNA site, higher concentrations of rhodium complex are required for effective competition. Instead, as also demonstrated in Figure 3, competitive titrations reveal extensive photocleavage at U24 by the rhodium complex at 20  $\mu\text{M}$  concentration. Therefore the rhodium complex does effectively compete with binding of the Tat peptide to its target.

### Discussion

The sites targeted by Rh(phen)<sub>2</sub>phi<sup>3+</sup> on BIV TAR RNA show a correspondence to those which are important in peptide binding and function. This is represented schematically in Figure 4. The strongest site is U24, a residue shown to be involved in triple base formation in the presence of BIV Tat peptide. Here we see that specific binding of the metal complex also depends upon base triple formation. Cleavage at U24 by the rhodium complex is abolished when the A13–U24 base pair is mutated to U13–A24 in the BIV1 RNA. This conservative mutation necessarily disrupts the base triple. This sequence is no longer recognized by the rhodium complex, probably because the major groove is no longer widened by the triple. Thus, the metal complex is sensitive to structural perturbations associated with this simple change in sequence. Remarkably the sensitivity of metal complex recognition to the base triple even exceeds that of the Tat peptide, where the U24A–A13U mutation produces 25% binding relative to wild type.<sup>1</sup>

Based upon the photocleavage data for the complex and the differential recognition of BIV TAR RNA versus BIV1, we would propose that the metal complex intercalates at the triple base site. Given that strand scission involves direct reaction of the activated phi ligand and the RNA, the phi ligand is likely to be stacked between the U10–A13–U24 triple and the G11–C25 base pair, in the widened major groove. Although the bulged site lacking the triple could provide some opening for the metal complex, given weak cleavage at G9 on BIV1, stacking against the triple base array provides critical stabilization of the intercalator in the fully folded site of BIV TAR RNA. The site is also likely to be a somewhat restricted one given the high enantioselectivity we observe. In the NMR structure of the TAR RNA bound by Tat peptide,<sup>3</sup> the width of the major groove at the G11–C25 base pair is thought to be 17 Å. These helical dimensions would likely allow access of the right-handed  $\Delta$ -Rh(phen)<sub>2</sub>phi<sup>3+</sup> for intercalation but not the  $\Lambda$ -isomer.<sup>14</sup> We cannot establish from these data whether the metal complex induces the conformational change of the RNA upon binding or whether, in the absence of metal complex as well as without peptide, the RNA adopts a folded form with triple base

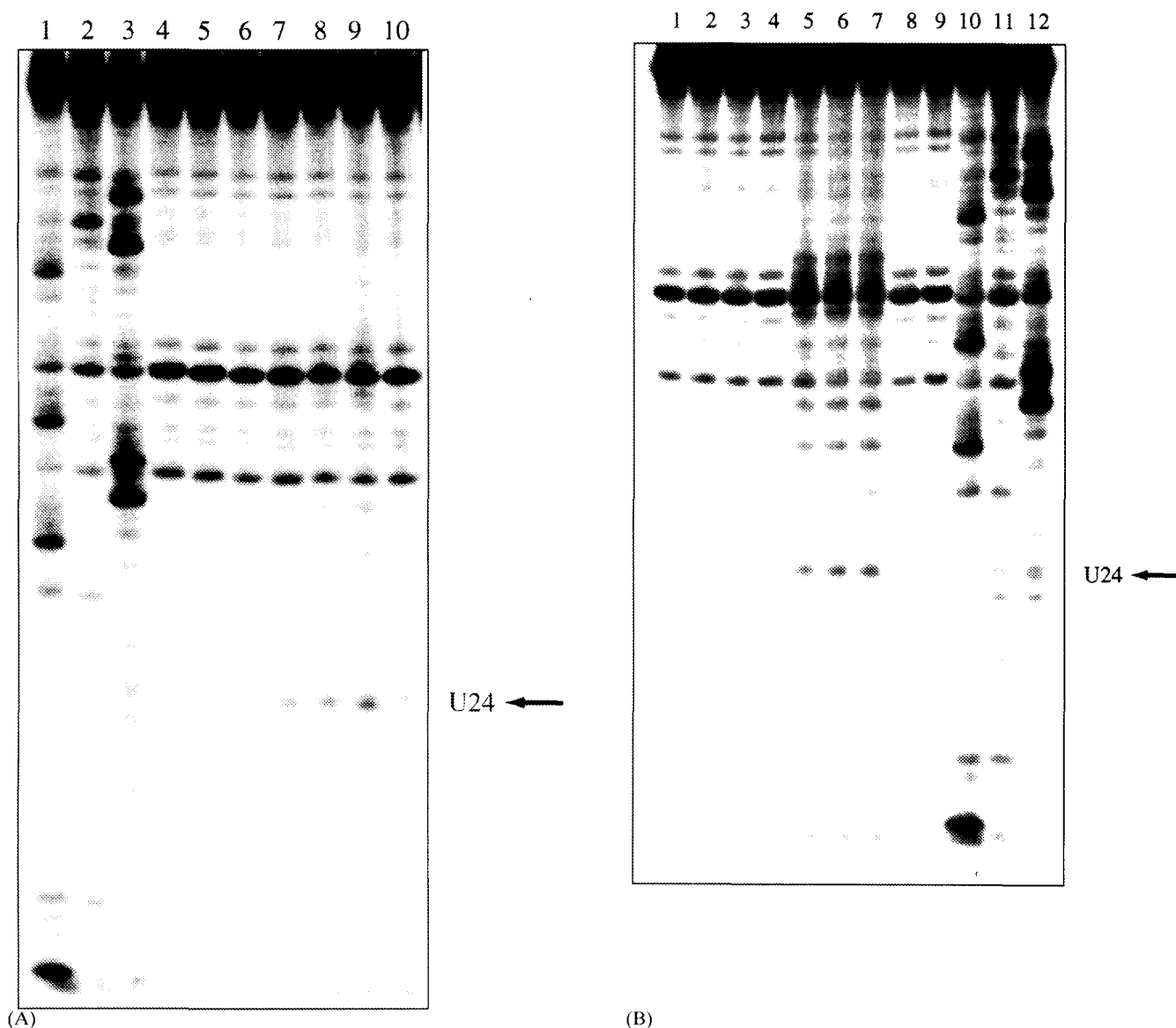


**Figure 3.** Competition for BIV TAR RNA between  $\text{Rh}(\text{phen})_3\text{phi}^{3+}$  and HIV (A) Tat peptide or BIV (B) Tat peptide. (A) Gray-scale representation of a phosphor autoradiogram of a 20% denaturing polyacrylamide gel showing  $\text{Rh}(\text{phen})_3\text{phi}^{3+}$  cleavage on  $3'$ - $^{32}\text{P}$ -labeled BIV RNA in 50 mM Tris-HCl, 18 mM NaCl, 10 mM NaOAc, pH 7.0. Lanes 1, 2, and 3: A-, G-, and U-specific reactions on BIV TAR RNA, respectively. Lanes 4, 5, 6, 7, 8, and 9: labeled BIV after incubation with 2  $\mu\text{M}$  HIV Tat and 0.1, 0.5, 1, 2, 5, and 10  $\mu\text{M}$   $\text{Rh}(\text{phen})_3\text{phi}^{3+}$ , respectively, and irradiation for 15 min at 365 nm. Lane 10: labeled BIV with 2  $\mu\text{M}$  HIV Tat and 5  $\mu\text{M}$   $\text{Rh}(\text{phen})_3\text{phi}^{3+}$ . (B) Gray-scale representation of a phosphor autoradiogram of a 20% denaturing polyacrylamide gel showing  $\text{Rh}(\text{phen})_3\text{phi}^{3+}$  cleavage on  $3'$ - $^{32}\text{P}$ -labeled BIV in 50 mM Tris-HCl, 18 mM NaCl, 10 mM NaOAc, pH 7.0. Lanes 1, 2, 3, 4, 5, 6, and 7: labeled BIV after incubation with 2  $\mu\text{M}$  BIV Tat and 1, 2, 5, 10, 25, 50, and 100  $\mu\text{M}$   $\text{Rh}(\text{phen})_3\text{phi}^{3+}$ , respectively, and irradiation for 15 min at 365 nm. Lane 8: labeled BIV with 2  $\mu\text{M}$  BIV Tat and 5  $\mu\text{M}$   $\text{Rh}(\text{phen})_3\text{phi}^{3+}$ . Lane 9: labeled BIV with 2  $\mu\text{M}$  BIV Tat upon irradiation for 15 min at 365 nm without metal. Lanes 10, 11, and 12: A-, G-, and U-specific reactions on BIV, respectively.

interaction. It is clear, however, that the same folded conformation required for peptide binding is required for recognition by the metal complex.

Perhaps most remarkable is the simple observation of high site-selectivity for the octahedral coordination complex, which lacks the array of functionalities present in the peptide and proposed to be critical for the peptide in achieving recognition of its nucleic acid site. Experiments in our laboratory have shown that the addition of guanidinium moieties to the ancillary ligands of the rhodium complex,<sup>15</sup> mimicking the

arginine side chains on the native peptide, may enhance to the same extent both the affinity and the selectivity of the metal complex for HIV and BIV RNA sequences.<sup>13</sup> However, as shown here, even without these functionalities, *shape-selection*, matching the shape of the small metal complex to its nucleic acid target, provides sufficient selective stabilization for RNA site discrimination. Indeed, we find that  $\text{Rh}(\text{phen})_3\text{phi}^{3+}$  competes effectively with the Tat peptide for its binding site on the TAR RNA. Our results therefore underscore once again the value of shape-selective recognition. Shape-selection can be powerfully applied not only in probing

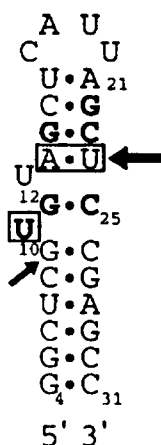


**Figure 4.** Schematic of the BIV TAR RNA showing the correspondence between nucleotides targeted by  $\text{Rh}(\text{phen})_2\text{phi}^{3+}$  cleavage (arrows with size corresponding to relative intensity) and those important for protein binding (bold) and tertiary folding (boxed).

structural variations along the nucleic acid polymer but also in the design of novel small molecules to target nucleic acid sites with high site-selectivity, in the development of molecules to inhibit protein recognition, and, potentially, in the design of new chemotherapeutics.

## Experimental

### RNA preparation

The BIV and BIV1 TAR RNAs were prepared by *in vitro* transcription<sup>16</sup> using synthetic DNA templates and T7 RNA polymerase (Pharmacia). DNA primer and template strands were synthesized on an ABI DNA 392 synthesizer, purified by reverse phase HPLC, detritylated, and purified again by HPLC. The RNA products from the transcription reactions were precipitated and washed with EtOH. The RNA oligomers were gel purified on an 8 or 10% polyacrylamide denaturing gel, located with UV shadowing, excised and then eluted from the gel using an Elutrap device (Schleicher and Schuell). After precipitation, the RNA was stored frozen in 10 mM Tris-HCl buffer pH 7.0 at  $-20^\circ\text{C}$ . The RNA oligomers were quantitated using UV-vis spectroscopy. The RNA oligomers were 3'-end-labeled with cytidine 3',5'-[5'- $^{32}\text{P}$ ]-bisphosphate using T4 RNA ligase.<sup>17</sup> They were purified and recovered as described for the unlabeled RNA. The eluted RNA oligomers were ethanol-precipitated twice and stored frozen in 10 mM Tris-HCl, pH 7.5.  $\text{Rh}(\text{phen})_2\text{phi}^{3+}$  solutions were prepared fresh in 10 mM Tris-HCl pH 7.0.

### Rhodium photocleavage

$[\text{Rh}(\text{phen})_2\text{phi}]\text{Cl}_3$  was prepared as described earlier.<sup>7</sup> The enantiomers were resolved by cation-exchange chromatography on a Sephadex SPC-25/potassium antimonate column.<sup>15</sup> All metal stock solutions were freshly prepared in either ethanol or 10 mM Tris-

HCl, pH 7.5. Photocleavage samples were prepared in buffer (50 mM Tris-HCl, 18 mM NaCl, 10 mM NaOAc, pH 7.0). A typical 20  $\mu\text{L}$  irradiation sample consisted of 50,000 cpm renatured  $^{32}\text{P}$ -labeled RNA, 0.001–10  $\mu\text{M}$  rhodium complex, 50 or 100  $\mu\text{M}$  nucleotides carrier TAR or  $\text{tRNA}^{\text{Phe}}$  in aqueous buffer. Rhodium complex was added to the sample 5–20 min before irradiation at ambient temperature at 365 nm on a 1000-W Hg/Xe lamp and monochromator (Oriel model 77250) for 5–20 min. The samples were precipitated, washed and dried, and then eluted through a 20% denaturing polyacrylamide gel. The full-length RNA oligomers and cleavage products were identified by coelectrophoresing with  $\text{Ru}(\text{phen})_3^{2+}$  (G-specific) reactions,<sup>18</sup> diethyl pyrocarbonate (DEPC) (A-specific) and hydrazine (U-specific) reactions.<sup>19</sup> The fragments produced by the metal complex cleavage possess 3'- and 5'-phosphate termini, and thus could be directly compared with the chemical sequencing lanes.<sup>8</sup>

### Determination of affinity constants

Binding constants were obtained through quantitative affinity cleavage titrations according to published procedures,<sup>20</sup> and experimental conditions as described above. The rhodium:RNA nucleotide ratio was held constant at 1:20. The bulk RNA used was tRNA from baker's yeast (Boehringer); previous experiments indicated that there is no difference in photocleavage sites and intensities between reactions done in the presence of tRNA or BIV RNA. The range of RNA concentrations used was 0.1–1000  $\mu\text{M}$ , while the rhodium complex ranged from 5 nM to 50  $\mu\text{M}$ . Photocleavage reactions were carried out at ambient temperature.

Affinity constants were determined in photocleavage experiments under single hit conditions, where

$$I_{\text{site}} = I_{\text{sat}} \frac{K_b [\text{RNA}]_{\text{site}}}{1 + K_b [\text{RNA}]_{\text{site}}}$$

and  $I_{\text{site}}$  is the intensity of photocleavage as measured by phosphorimager,  $I_{\text{sat}}$  is the intensity of photocleavage at saturating rhodium concentration,  $K_b$  is the affinity constant, and  $[\text{RNA}]_{\text{site}}$  is the concentration of RNA hairpins.

Quantitation was accomplished using photostimulable storage phosphorimaging Kodak screens S0230 from Molecular Dynamics. A Molecular Dynamics 400S PhosphorImager was used to scan the screens, and Imagequant version 3.3 was used to analyze the data.

### Peptide preparation

The nine-mer RKKRRQRRRC and the 14-mer RPRGTRGKGRIR peptides derived from the HIV Tat and BIV Tat peptides, respectively, were chemically synthesized and purified by the Biopolymer Synthesis and Analysis Resource Center at Caltech. The peptides were prepared as their COOH-terminus amides, and

the HIV Tat peptide was acetylated on the NH<sub>2</sub> terminus. The peptides were analyzed by capillary electrophoresis and mass spectrometry. The peptides were suspended in 10 mM Tris-HCl pH 7.0 and stored frozen until use.

### Competition experiments with Tat peptide

Rhodium competition experiments were carried under the same conditions for photocleavage, with the addition of either BIV or HIV Tat peptide to the photocleavage solutions. Experiments were carried out with either a fixed concentration of rhodium complex with the peptide concentrations varied, or with a fixed concentration of peptide and varying the rhodium concentration. In both cases, all components except for the rhodium complexes were allowed to equilibrate for 1 h, before the addition of the rhodium complex and subsequent irradiation. All competition experiments were carried out at ambient temperature.

### Acknowledgements

We are grateful to the National Institute of General Medical Sciences (GM33309) for their financial support of this research. In addition we thank Glaxo Research for fellowship support (A.C.L.).

### References

1. Chen, L.; Frankel, A. D. *Biochemistry* **1994**, *33*, 2708.
2. Puglisi, J. D.; Chen, L.; Blanchard, S.; Frankel, A. D. *Science* **1995**, *270*, 1200.
3. Ye, X.; Kumar, R.A.; Patel, D.J. *Current Biology* **1995**, *2*, 827.
4. Puglisi, J. D.; Tan, R.; Calnan, B.J.; Frankel, A. D.; Williamson, J. R. *Science* **1993**, *257*, 76.
5. Johann, T. W.; Barton, J. K. *Phil. Trans. Royal Soc. A* **1996**, *354*, 299.
6. David, S. D.; Barton, J. K. *J. Am. Chem. Soc.* **1993**, *115*, 2984.
7. Chow, C. S.; Barton, J. K. *Meth. Enzym.* **1992**, *212*, 219.
8. Sitlani, A.; Long, E. C.; Pyle, A. M.; Barton, J. K. *J. Am. Chem. Soc.* **1992**, *114*, 2303.
9. Chow, C. S.; Behlen, L. S.; Uhlenbeck, O. C.; Barton, J. K. *Biochemistry* **1992**, *31*, 972.
10. Campisi, D.; Morii, T.; Barton, J. K. *Biochemistry* **1994**, *33*, 4130.
11. Lim, A.C.; Barton, J. K. *Biochemistry* **1993**, *32*, 11029.
12. Neenhold, H. R.; Rana, T. M. *Biochemistry* **1995**, *34*, 6303.
13. Lim, A. C. unpublished results.
14. Barton, J. K. *Science* **1986**, *233*, 727.
15. Terbrueggen, R. H.; Barton, J. K. *Biochemistry* **1995**, *34*, 8227.
16. Miligan, J. F.; Groebe, D. R.; Witherall, G. W.; Uhlenbeck, O. C. *Nucleic Acids Res.* **1987**, *15*, 8783.
17. England, T. E.; Uhlenbeck, O. C. *Nature* **1978**, *275*, 560.
18. Chow, C. S.; Barton, J. K. *J. Am. Chem. Soc.* **1990**, *112*, 2839.
19. Peattie, D. A. *Proc. Natl. Acad. Sci. U.S.A.* **1979**, *76*, 1760.
20. Singleton, S. F.; Dervan, P. B. *Biochemistry* **1992**, *31*, 10995.

(Received in U.S.A. 10 September 1996; accepted 18 February 1997)